Self- and interdiffusion in dilute liquid germanium-based alloys

OPEN ACCESS
IOP Publishing
Journal of Physics: Condensed Matter
J. Phys.: Condens. Matter **31** (2019) 455101 (6pp)
https://doi.org/10.1088/1361-648X/ab354e

Self- and interdiffusion in dilute liquid germanium-based alloys

H Weis[1], F Kargl[1], M Kolbe[1], M M Koza[2], T Unruh[3,4] and A Meyer[1]

[1] Institut für Materialphysik im Weltraum, Deutsches Zentrum für Luft- und Raumfahrt (DLR), 51170 Köln, Germany
[2] Institut Laue-Langevin, CS 20156, 38042 Grenoble Cedex 9, France
[3] Forschungsneutronenquelle Heinz Maier-Leibnitz (FRM II), Technische Universität München, 85747 Garching, Germany

E-mail: andreas.meyer@dlr.de

Received 16 May 2019, revised 15 July 2019
Accepted for publication 22 July 2019
Published 19 August 2019

Abstract

Self- and inter-diffusion coefficients in liquid Ge and dilute Ge-based Ge–Si, Ge–Au, Ge–In, Ge–Ce and Ge–Gd alloys-containing 2 at% additions, respectively, are measured using a comprehensive approach of measuring techniques: quasi-elastic neutron scattering, *in situ* long-capillary experiments combined with x-ray radiography, and a long-capillary experiment under microgravity conditions. Resulting inter- and Ge self-diffusion coefficients are equal within error bars for each investigated alloy. The interdiffusion coefficients are smaller for the alloys containing Ce and Gd, However, no dependence of the atomic mass of the minor additions, that varies by about a factor of seven between Si and Au, on the diffusion coefficients could be observed. This demonstrates that in a loosely-packed metallic liquid with fast diffusive dynamics the diffusion mechanism is highly collective in nature.

Keywords: self diffusion, solute diffusion, liquid germanium, quasielastic neutron scattering, long-capillary, x-ray radiography, microgravity

(Some figures may appear in colour only in the online journal)

1. Introduction

In crystalline silicon and germanium diffusion coefficients of impurities or dopants differ by orders of magnitude as a result of vacancy-mediated diffusion mechanisms [1, 2]. Upon melting both silicon and germanium undergo a semiconductor to metal transition which comes along with an increase in density. In germanium the density increase from crystalline to liquid germanium at the melting point is about 5%. Despite of this and as compared to other liquid metals, liquid germanium is loosely packed and exhibits an averaged nearest neighbor coordination number of about 5.6 [3]. A similar picture is found in liquid silicon [4, 5]. In liquid silicon and germanium little is known about the mobility of minor additions and their impact on the overall self diffusivity of silicon and germanium, respectively. Experimental data are scarce and scatter by nearly one order of magnitude.

In densely packed metallic liquids, like nickel or iron the nearest neighbor coordination number is about 12 [6]. Here, e.g. the addition of carbon to liquid iron [7], phosphorus or aluminum to liquid nickel [8, 9] only has a minor effect on the self diffusion of iron or nickel, respectively. This behavior can be understood in terms of a highly collective transport mechanism, where caging becomes dominant [10]. As a consequence the self-diffusion coefficients of the various components in an alloy are similar [11–13] and the isotope effect, which is a measure of the dependence of mass of the diffusing atom, is close to zero [14]. In simple, loosely-packed liquids, binary collisions of individual hard-sphere like particles are envisioned as the prominent diffusion mechanism [15–17]. There, a dependence of the square root of the mass of the

[4] Present address: Lehrstuhl für Kristallographie und Strukturphysik, Friedrich-Alexander-Universität Erlangen-Nürnberg, 91058 Erlangen, Germany

diffusing particle is expected for the diffusion coefficient and the isotope effect is unity. Again experimental diffusion data are scarce. Measurements aboard the space shuttle on liquid tin report an isotope effect of about 0.3 at the melting temperature, that is increasing to about 0.7 with increasing temperature [18].

Here, we provide accurate experimental data on self- and interdiffusion in liquid germanium with various minor additions (2% of silicon, gold, indium, gadolinium, and cerium), in order to address how such minor additions affect the overall mobility of the germanium atoms. By studying minor additions of different atomic size and mass, we discuss on how interdiffusion is related to the self diffusion of the Ge atoms and to the self-diffusion coefficients of the minor additions. We have measured the self-diffusion of germanium both in pure germanium and in the Ge-based alloys with quasielastic neutron scattering and the interdiffusion in liquid $Ge_{98}X_2$ with X = Au, In, Gd, and Ce *in situ* with x-ray radiography. Due to the insufficient x-ray radiography contrast and the absence of a stable density layering, the interdiffusion measurement on $Ge_{98}Si_2$ was performed *ex situ* under microgravity conditions aboard the MAPHEUS sounding rocket. In microgravity density-driven fluid flow effects are suppressed [19].

Available measurements of diffusion coefficients are often hampered by convective contributions to mass transport during annealing as well as by artifacts from melting and solidification of the samples. E.g. in liquid germanium close to the melting point of 1211 K data range from 2.1×10^{-8} m^2 s^{-1} from an elaborated long-capillary (LC) diffusion experiment on solute gallium diffusion using a shear-cell [20] to a value of 2.8×10^{-9} m^2 s^{-1} estimated from segregation of gallium during growth of germanium crystals ([21] and references therein); In pure liquid germanium a capillary tracer experiment lists self-diffusion coefficients that range from 0.66×10^{-8} m^2 s^{-1} to 3.2×10^{-8} m^2 s^{-1} in a temperature range from 1233 K to 1493 K [22]. It has recently been shown with x-ray radiography on ground and in space, that accurate interdiffusion data can be measured in a long-capillary set-up by *in situ* monitoring of the diffusion process [23, 24]. In the case of self diffusion, incoherent quasielastic neutron scattering (QNS) has proven to be a versatile tool for the accurate measurement of atomic mobilities. Neutron scattering probes the diffusive dynamics on microscopic time and length scales and, therefore, quasielastic spectra are not altered by fluid flow effects [25]. Furthermore, it has been shown, that even for small incoherent cross sections and/or a large ratio of coherent to incoherent scattering, quasielastic neutron scattering allows to obtain accurate self-diffusion coefficients. Applied to pure liquid germanium scattering of a sample with natural isotopic abundance and of a sample containing 50% ^{73}Ge isotope, yielded the same self-diffusion coefficient within error bars, although the ratio of coherent to incoherent scattering varies by an order of magnitude between the samples [26]. Silicon has a vanishing incoherent scattering cross section. Quasielastic neutron scattering on Si–Ni alloys containing 5 at%, 10 at% and 20 at% Ni, respectively, therefore,

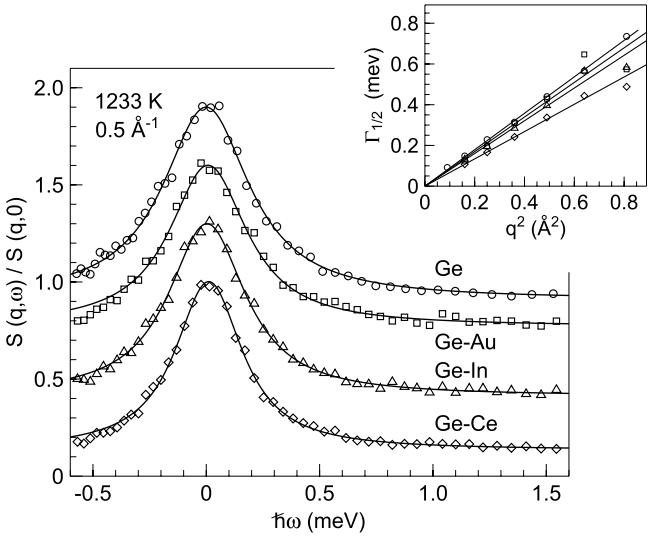

Figure 1. Quasielastic spectra $S(q, \omega)$ of pure liquid germanium and $Ge_{98}X_2$ alloys with X = Au, In, Ce. For clarity the spectra are shifted by 0.3 each. The lines are fits with equation (2). Inset: line width as a function of q^2. The lines are fits with equation (3).

allowed to obtain the self-diffusion coefficients of nickel [27]. Resulting values in Si–Ni are equal within error bars, and are a factor of about five larger than in pure liquid nickel.

In binary liquids with a concentration of C_1 and C_2 the interdiffusion coefficient $D_{\rm int}$ is related to the self-diffusion coefficients of the two components $D_{\rm s1/2}$ via an extension of the Darken equation [28]:

$$D_{\rm int} = (C_1 D_{\rm s2} + C_2 D_{\rm s1})\, \Phi\, S, \qquad (1)$$

where Φ is the thermodynamic factor and S a factor that takes cross-correlations into account. Toward small concentration C_2, Φ, S and C_1 become unity and, hence, $D_{\rm int} \simeq D_{\rm s2}$ [23]. Therefore, the interdiffusion coefficients presented here represent in good approximation the self-diffusion coefficients of the minor addition, i.e. the solute element.

2. Experimental

The temperature dependence of the self-diffusion in pure liquid Ge was measured on the neutron time-of-flight spectrometer ToFToF at the Forschungsneutronenquelle Heinz Maier-Leibnitz. For the experiment a sample of a 1:1 isotope mixture of high purity $^{\rm nat}$Ge and ^{73}Ge was prepared. The isotope-mixture yields an incoherent scattering cross section of $\sigma_{\rm inc} = 1.2$ barn, that is significantly larger than that of $^{\rm nat}$Ge with $\sigma_{\rm inc} = 0.18$ barn [29]. Samples were filled into thin walled Al_2O_3 cylinders giving a hollow cylindrical sample geometry of 22 mm in diameter, 1.2 mm in wall thickness, and 40 mm in height. An incoming neutron wavelength of $\lambda = 7$ Å gave an accessible wavenumber range of $(0.3 < q < 1.6)$ Å^{-1} with an instrumental energy resolution of about 50 μeV at full width at half maximum. Measurements were performed inside a standard niobium resistance furnace in a temperature range between 1223 K–1520 K.

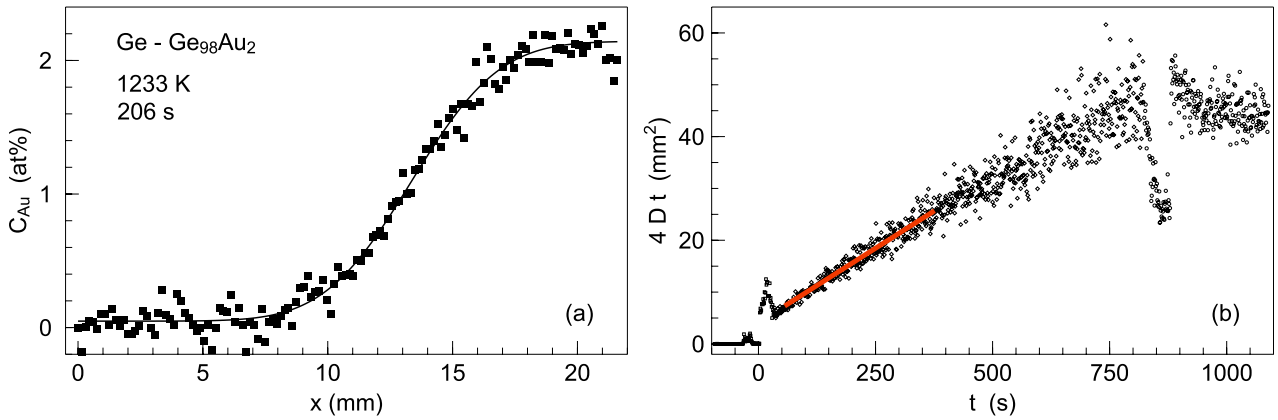

Figure 2. (a) Au-concentration profiles for the diffusion couple Ge − $Ge_{98}Au_2$ obtained from time resolved x-ray radiography at 206 s. The line is fit with equation (4). (b) Diffusion length squared $L^2 = 4Dt$ derived from fits depicted in (a) as a function of time. The red line represents a linear fit to the time range, where steady state conditions have been reached, diffusion profiles are free from artifacts, and equation (4) is valid.

Quasielastic neutron scattering on liquid $Ge_{98}X_2$ (with X = Au, In, and Ce) was performed on the crystal time-of-flight spectrometer IN6 at the Institut Laue-Langevin. Here an incoming neutron wavelength of $\lambda = 5.1$ Å gave an accessible wavenumber range of $(0.4 < q < 2.0)$ Å^{-1} with an instrumental energy resolution of about 70 μeV at full width at half maximum. Note that QNS measurements of GeGd are prevented by the huge absorption cross section of Gd [29]. The alloys were prepared by arc melting of high purity materials and subsequently filled in thin walled Al_2O_3 cylinders, giving a cylindrical sample shape of 9 mm in diameter and 40 mm in length. The samples were processed at a single temperature of 1233 K close to the Ge melting point at $T_m = 1211$ K for 2 h each.

The neutron scattering data were normalized to a vanadium standard, corrected for self-absorption and empty container scattering and interpolated to constant q in order to obtain the dynamic structure factor $S(q,\omega)$ (figure 1). For the data analysis the FRIDA program has been used [30]. All quasielastic spectra are well described by a single Lorentz function:

$$F(q,\omega) = \frac{A}{\pi}\frac{\Gamma_{1/2}(q)}{(\hbar\omega)^2 + \Gamma_{1/2}^2(q)} \otimes R(q,\omega) + b(q) \qquad (2)$$

convolved with the instrumental energy resolution function $R(q,\omega)$, that was measured with a vanadium standard of sample size. Here, $b(q)$ denotes an energy independent background and $\Gamma_{1/2}(q)$ the half width at half maximum of the Lorentz function. $\Gamma_{1/2}(q)$ is proportional to the germanium self-diffusion coefficient according to [25, 31]:

$$D_s = \frac{\Gamma_{1/2}(q)}{\hbar q^2}. \qquad (3)$$

It is important to note, that none of the minor additions exhibits an incoherent scattering cross section larger than 0.54 barn. Taking into account the solute content in the alloy of only 2 at%, the quasielastic signal is dominated by the incoherent scattering contribution of Ge, and, hence, the Ge self-diffusion coefficient can be obtained via equations (2) and (3).

The interdiffusion experiments were performed in thin graphite capillaries giving a sample diameter of 1.3 mm. Rod-shape samples of 15 mm in length were produced: (i) by ultrasonic drilling from an ingot in the case of Ge; and (ii) by arc melting of Ge and the respective component in a high purity Argon atmosphere followed by suction casting into a water cooled copper mold of appropriate dimensions. Interdiffusion in liquid Ge–GeAu, Ge–GeIn, Ge–GeGd and Ge–GeCe was measured using the long-capillary technique in combination with *in situ* imaging of diffusion profiles using x-ray radiography [32]. X-ray images of the diffusion couple including the furnace were taken during the entire diffusion experiment with a time resolution of one second. The samples were heated with a constant heating rate of about 3.4 K s^{-1}. The temperature gradient along the sample was less than 0.5 K at the annealing temperature of 1233 K. A detailed description of the experimental setup including an explanation of the data analysis is given in [33].

From the time dependent x-ray images solute concentration profiles were deduced, exemplary for the Ge–$Ge_{98}Au_2$ diffusion couple depicted in figure 2(a). The solute concentration profiles are well described by:

$$C(x,t) = \frac{C_1 + C_2}{2} + \frac{C_1 - C_2}{2} \cdot \text{erf}\left(\frac{x - x_0}{\sqrt{4Dt}}\right), \qquad (4)$$

as the appropriate solution of the diffusion equation [34]. Here C_1 and C_2 represent the end concentrations of the diffusion couple and x_0 the center of the diffusion zone. The diffusion length squared $L^2 = 4Dt$ is shown in figure 2(b). *In situ* x-ray monitoring enables the real-time analysis of concentration profiles in 2 dimensions. This in particular allows us to exclude data where gas bubbles or free surfaces causing Marangoni convection hamper the measurement [35]. For the Ge–$Ge_{98}X_2$ (with X = Au, In, Cd, Ce) diffusion couples a stable density layering suppressed gravity driven fluid flow effects. For the analysis of the diffusion coefficients only times are taken into account at which the temperature inside the furnace is constant, the sample is fully liquid, mass transport is solely diffusive, and the diffusion process has not progressed to an extend

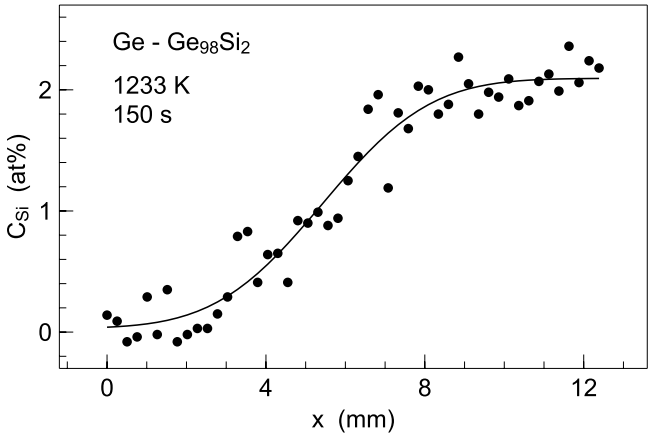

Figure 3. Si-concentration profile of the solidified Ge–$Ge_{98}Si_2$ diffusion couple, annealed under microgravity conditions. The atomic concentrations were measured using energy dispersive x-ray analysis on polished surfaces parallel to the rotation axis of the diffusion couple. The line is a fit with equation (4) as the appropriate solution of the diffusion equation.

where the initial concentrations towards the sample ends changed. Figure 2(b) displays a typical developing of L^2 as a function of time. Up to $t \equiv 0$ the sample is solid. Below about 30 s, solute concentration profiles are hampered by melting of the sample. Then up to about 400 s a steady state diffusion process leads to a linear dependence of L^2, before first the progressing interdiffusion leads to a change in the end concentrations, and, second the samples solidifies at about 820 s.

Along the Ge–$Ge_{98}Si_2$ diffusion couple virtually no density gradient exits, which prevents measurements on ground due to a missing stable density layering that suppresses density driven convective flow [19]. The interdiffusion in Ge–$Ge_{98}Si_2$ was therefore measured in a long-capillary (LC) experiment inside a vacuum chamber aboard the MAPHEUS sounding rocket, which provided reduced gravity of 10^{-4} g for a time of 200 s. A detailed description of the experimental setup is given in [36]. The sample was heated with a rate of 7 K s^{-1} to 1233 K, at which diffusion annealing took place for 150 s. Subsequently, it was cooled by flooding the vacuum chamber with He-gas, resulting in a cooling rate of 6 K s^{-1}. The sample was fully solidified before the end of the microgravity phase.

Ge–$Ge_{98}Si_2$ is well suited for *ex situ* diffusion experiments in microgravity, since in the diffusion couple liquidus and solidus temperatures differ by less than 20 K and Si is fully miscible in Ge [37]. Hence, artifacts from melting and solidifying in the sample are expected to be small. This is also shown by scanning electron microscopy of the annealed sample that revealed no concentration shifts, e.g. due to formation of voids or bubbles, or due to solid state phase formation. The Si- and Ge-concentrations along the sample were measured using energy dispersive x-ray analysis (EDX). Although the density difference between the solid sample at room temperature and the annealing temperature in the liquid is less than 5%, no change in sample length has been observed. During solidification the liquid is pushed into the graphite wall. For this reason no length correction has been performed. Figure 3 shows the Si-concentration along the diffusion profile. Data are well described by equation (4).

3. Results and discussion

In pure liquid germanium the resulting self-diffusion coefficients range from $1.34(7) \times 10^{-8}$ m^2 s^{-1} at 1223 K to $1.77(11) \times 10^{-8}$ m^2 s^{-1} at 1520 K. These values are significantly larger than self-diffusion coefficients of pure liquid iron (2.8×10^{-9} m^2 s^{-1} at 1811 K [7]) and pure liquid nickel (3.3×10^{-9} m^2 s^{-1} at 1728 K [38]) at the respective melting temperatures. The temperature dependence is well described by an Arrhenius law: $D = D_0 \exp(-E_A/(k_B T))$ with an activation energy of $E_A = 156 \pm 17$ meV and a prefactor $D_0 = 5.9(7) \times 10^{-8}$ m^2 s^{-1}. $k_B = 8.617 \times 10^{-2}$ meV K^{-1} is the Boltzmann constant. Data are shown in figure 4 [39][5]. As compared to liquid iron ($E_A = 540 \pm 34$ meV) and liquid nickel ($E_A = 470 \pm 30$ meV) the activation energy in liquid germanium is about a factor of three smaller. The values of the germanium self-diffusion coefficients, however, compare well with the quasielastic neutron scattering values of nickel self diffusion in the Si–Ni alloys [27]: at the melting temperature of liquid silicon D_{Ni} is about $1.4(1) \times 10^{-8}$ m^2 s^{-1}. The activation energy of liquid Si–Ni $E_A = 280 \pm 20$ meV is, however, significantly larger than in pure germanium.

Figure 4 displays the self- and interdiffusion coefficients determined in this work. Where measured (GeAu, GeIn, and GeCe), Ge self-diffusion and interdiffusion coefficients are equal within error bars. We note, that a QNS experiment on liquid $Ge_{80}Si_{20}$ resulted in a Ge self-diffusion coefficient that is equal within error bars to pure liquid germanium [40]. Even the addition of 20 at% Si to Ge has no impact on the atomic mobility of the Ge atoms. Hence, in reasonable approximation, also the addition of 2 at% Si to Ge does not affect the self diffusion of Ge. For Ge–Au, Ge–In and Ge–Si, measured self- and interdiffusion coefficients are also equal within error bars to the Ge self-diffusion coefficient in pure liquid Ge. In Ge–Ce and Ge–Gd, on the other hand, diffusion coefficients are smaller by up to a factor of 2 compared to pure liquid Ge. The addition of 2 at% Si, Au or In has no impact on the mobility of the germanium atoms, whereas the addition of 2 at% Ce also slows down the overall dynamics of the liquid, as seen by a smaller Ge self-diffusion coefficient.

Comparing the covalent radii they are significantly larger for Gd (1.96 Å) and Ce (2.04 Å) than for Ge (1.2 Å), Au (1.36 Å), In (1.42 Å), and Si (1.11 Å). From our study we cannot infer to what extent the chemical interactions in such a dilute system play a role. In a Ce-based glass forming alloy, the addition of 1 at% niobium, leads to a significant slowing down of the overall diffusive dynamics in the melt [41]. There, it appears that this is not triggered by a large atomic size of the minor addition,

[5] We note that data on self diffusion in liquid germanium have been published before [39]. In that experiment a graphite cylinder was used as a sample holder that gives significant scattering contributions to the quasielastic signal. As a consequence the resulting line widths are about 20% larger at the melting point than values reported here and also exhibit a different temperature dependence. In addition, Chathoth *et al* miscalculated the diffusion coefficients from the line width by a factor of about 1.5, which is close to the prefactor of 1.517 of $1/\hbar$ in $D = \Gamma_{1/2}(q)/(\hbar q^2)$ with $\hbar = 0.659 \times 10^{-15}$ meV s. As a consequence, values in [39] for the Ge self-diffusion coefficients are systematically smaller than the real values and their temperature dependence exhibits a larger activation energy.

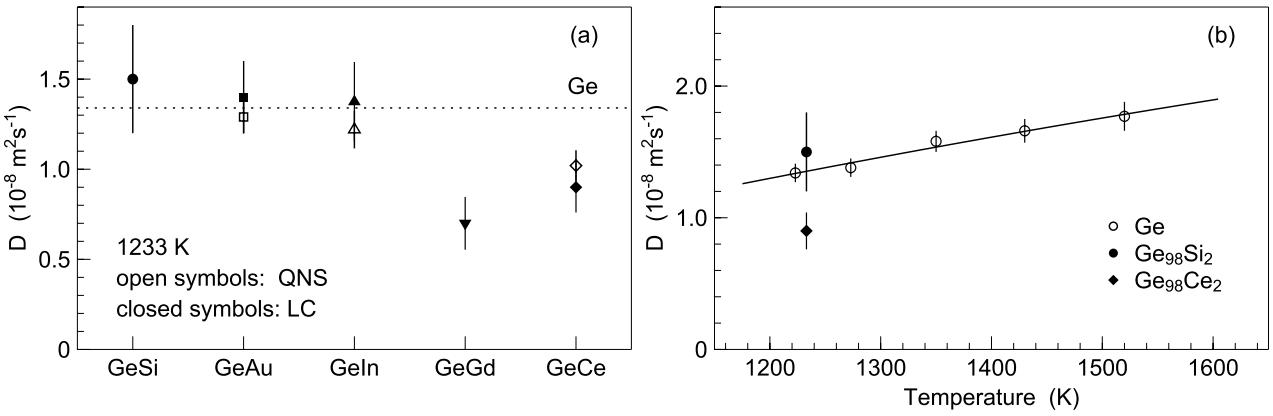

Figure 4. (a) Ge self-diffusion in liquid $Ge_{98}X_2$, (X = Au, In, Ce) from quasielastic neutron scattering (QNS) and interdiffusion coefficients in $Ge_{98}X_2$, X = Si, Au, In, Ce, Gd diffusion couples from long-capillary (LC) experiments. The dashed line represents the Ge self-diffusion coefficient in pure Ge. (b) Ge self-diffusion coefficient as a function of temperature. The line is a fit with an Arrhenius law. Two LC data points from (a) are included.

since Nb has a covalent radius of about 1.34 Å, which is significantly smaller than that of the main component Ce.

Following the discussion above, at small solute concentrations the main contribution to the interdiffusion coefficient is due to the self-diffusion of the minor addition. Hence, the interdiffusion coefficients shown here represent in good approximation the self-diffusion coefficients of the solute element. Their atomic masses range from 197 u for Au to 28.1 u for Si (Ge: 72.6 u). Apparently, a change of mass by a factor of about seven has no impact on the mobility of the solute. In liquids, a dependence on the square root of mass of the diffusive particle is expected for the diffusion coefficient for diffusion mechanisms based on hopping processes of individual particles, or on binary collisions of hard-spheres [15–17]. On the contrary, in a glass-forming metallic melt tracer diffusion experiments revealed a vanishing isotope effect [14], i.e. also no dependence on mass. In such a densely-packed liquid, where, however, the diffusion coefficients of the various components at the liquidus temperature are about two orders of magnitude smaller than in liquid Ge [12], diffusive transport of mass relies on a highly collective mechanism.

In this context, liquid germanium serves as prime example of a high-temperature, loosely-packed liquid, with fast atomic mobility. For such a liquid kinetic theories predict transport in the hydrodynamic regime to be governed by uncorrelated binary collisions of atoms, and, hence, a self-diffusion coefficient that is inversely proportional to the square root of the atomic mass [15–17]. The absence of any influence of atomic mass on the self-diffusion coefficients of the minor additions reported here, however, demonstrates that the picture of hard-sphere like binary collisions does not apply to liquid germanium. These findings are in line with *ab initio* molecular dynamics simulations in liquid Ge models, that show that diffusive transport cannot be described within Enskog theory [42] and that exhibit the existence of a microscopic cage effect [43].

4. Conclusions

We present measurements of self- and interdiffusion coefficients in liquid Ge and Ge-based Ge–Au, Ge–In, Ge–Ce, Ge–Gd and Ge–Si melts. Special care has been taken to ensure that the measurements are not hampered by convective contributions to mass transport. This is achieved by the use of quasielastic neutron scattering, *in situ* monitoring of the diffusion process with x-ray radiography and an experiment under microgravity conditions. The self-diffusion coefficient in pure liquid germanium at the melting temperature is 1.3×10^{-8} m^2 s^{-1}, which is about a factor of 4 larger than in liquid nickel at its melting temperature. At the same time, the activation energy $E_A = 156 \pm 17$ meV, is about a factor 3 smaller as compared to liquid nickel. Although the combination of fast diffusion dynamics and low activation energy may suggest transport via an uncorrelated single-particle process, the resulting self- and interdiffusion coefficients show no decoupling of the mobility of the minor additions from that of the surrounding Ge atoms. Furthermore, in contradiction to kinetic theories that describe self diffusion in liquid metals by a mechanism that is based upon binary collisions, the diffusion coefficients reported here are independent of the atomic mass of the diffusing species, indicating a highly collective transport mechanism.

Our results in liquid germanium show, that in good approximation the self-diffusion coefficient of the solute element is similar to the overall self diffusion of the germanium melt. Although the addition of 2 at% Gd or Ce also impacts the self diffusion of the germanium in the alloy by up to 50%, values for the Si, In and Au solute diffusion-coefficients do not scale with their atomic mass, and within errors bars also not with their covalent atomic radius. Therefore, the solute diffusion-coefficients in liquid germanium cannot be calculated with existing models that predict a mass and/or size dependence. The results on Ni self

diffusion in liquid Si–Ni at low Ni content indicate [27], that a similar picture may also hold for solute diffusion in liquid silicon. To what extent these findings also apply to other solute elements in liquid silicon and germanium, and to solute diffusion in other more densely-packed liquid metals, like iron or nickel, in general, can now be accurately investigated with *in situ* monitoring of the diffusion with x-ray or neutron radiography [44].

Acknowledgment

We thank Thomas Voigtmann and Dirk Holland-Moritz for a critical reading of the manuscript and Axel Griesche for his introduction to advanced long-capillary diffusion experiments on ground and in space.

ORCID iDs

A Meyer https://orcid.org/0000-0002-0604-5467

References

[1] Chroneos A and Bracht H 2014 *Appl. Phys. Rev.* **1** 011301
[2] Gösele U M 1988 *Annu. Rev. Mater. Sci.* **18** 257
[3] Salmon P 1988 *J. Phys. F: Met. Phys.* **18** 2345
[4] Ansell S, Krishnan S, Felten J J and Price D L 1998 *J. Phys.: Condens. Matter* **10** L73
[5] Kimura H *et al* 2001 *Appl. Phys. Lett.* **78** 604
[6] Schenk T, Holland-Moritz D, Simonet V, Bellissent R and Herlach D M 2002 *Phys. Rev. Lett.* **89** 075507
[7] Meyer A, Hennig L, Kargl F and Unruh T 2019 *J. Phys.: Condens. Matter* **31** 395401
[8] Mavila Chathoth S, Meyer A, Schober H and Juranyi F 2004 *Appl. Phys. Lett.* **85** 4881
[9] Stüber S, Holland-Moritz D, Unruh T and Meyer A 2010 *Phys. Rev.* B **81** 024204
[10] Meyer A 2002 *Phys. Rev.* B **66** 134205
[11] Griesche A, Macht M-P, Suzuki S, Kraatz K-H and Frohberg G 2007 *Scr. Mater.* **57** 477
[12] Bartsch A, Rätzke K, Meyer A and Faupel F 2010 *Phys. Rev. Lett.* **104** 195901
[13] Basuki S W, Yang F, Gill E, Rätzke K, Meyer A and Faupel F 2017 *Phys. Rev.* B **95** 024301
[14] Zöllmer V, Rätzke K, Faupel F and Meyer A 2003 *Phys. Rev. Lett.* **90** 195502
[15] Kirklady J S and Young D S 1987 *Diffusion in the Condensed State* (London: Institute of Metals)
[16] Iida T and Guthrie R I L 1988 *The Physical Properties of Liquid Metlas* (Oxford: Clarendon)
[17] Hansen J-P and McDonald I R 2006 *Theory of Simple Liquids* (New York: Academic)
[18] Frohberg G, Kraatz K-H and Wever H 1987 *Mater. Sci. Forum* **15–8** 529
[19] Barat C and Garandet J P 1996 *Int. J. Heat Mass Transfer* **39** 2177
[20] Bourret E D, Favier J J and Bourrel O 1981 *J. Electrochem. Soc.* **128** 2473
[21] Garandet J P 2008 *J. Cryst. Growth* **310** 3268
[22] Pavlov P V and Dobrokhotov E V 1970 *Sov. Phys. Solid State* **12** 225
[23] Sondermann E, Kargl F and Meyer A 2016 *Phys. Rev.* B **93** 184201
[24] Sondermann E, Jakse N, Binder K, Mielke A, Heuskin D, Kargl F and Meyer A 2019 *Phys. Rev.* B **99** 024204
[25] Meyer A 2015 *EPJ Web Conf.* **83** 1002
[26] Weis H, Unruh T and Meyer A 2013 *High Temp. High Press.* **42** 39
[27] Pommrich A I, Meyer A, Holland-Moritz D and Unruh T 2008 *Appl. Phys. Lett.* **92** 241922
[28] Horbach J, Das S K, Griesche A, Frohberg G, Macht M-P and Meyer A 2007 *Phys. Rev.* B **75** 174304
[29] Koester L, Rauch H and Seymann E 1991 *At. Data Nucl. Data Tables* **49** 65
[30] FRIDA-1: http://sourceforge.net/projects/frida
[31] Boon J P and Yip S 1980 *Molecular Hydrodynamics* (New York: McGraw-Hill)
[32] Zhang B, Griesche A and Meyer A 2010 *Phys. Rev. Lett.* **104** 035902
[33] Griesche A, Zhang B, Solórzano E and Garcia-Moreno F 2010 *Rev. Sci. Instrum.* **81** 056104
[34] Crank J 1975 *The Mathematics of Diffusion* (New York: Oxford University Press)
[35] Kargl F, Sondermann E, Weis H and Meyer A 2013 *High Temp. High Press.* **42** 3
[36] Blochberger G, Drescher J, Neumann C, Penkert P, Griesche A, Kargl F and Meyer A 2011 *J. Phys.: Conf. Ser.* **327** 012051
[37] Massalski T B 1990 *Binary Alloy Phase Diagrams* (Ohio: ASM International)
[38] Meyer A, Stüber S, Holland-Moritz D, Heinen O and Unruh T 2008 *Phys. Rev.* B **77** 092201
[39] Chathoth S M, Damaschke B, Unruh T and Samwer K 2009 *Appl. Phys. Lett.* **94** 221906
[40] Weis H 2012 Struktur- und Dynamik in flüssigem Germanium und Silizium–Germanium *PhD Dissertation* Ruhr-Universität Bochum
[41] Chathoth S M, Damaschke B, Embs J P and Samwer K 2009 *Appl. Phys. Lett.* **95** 191907
[42] Hugouvieux V, Farhi E, Johnson M R, Juranyi F, Bourges P and Kob W 2007 *Phys. Rev.* B **75** 104208
[43] Munejiri S, Masaki T, Itami T, Shimojo F and Hoshino K 2008 *Phys. Rev.* B **77** 014206
[44] Kargl F, Engelhardt M, Yang F, Weis H, Schmakat P, Schillinger B, Griesche A and Meyer A 2011 *J. Phys.: Condens. Matter* **23** 254201